SYSTEMATIC PREPARATION AND PHYSICAL PROPERTY CHARACTERIZATION OF A NOVEL STABLE $BiOIO_3$ NANOFLUIDS

by

Ruihao ZHANG, Hao ZHANG, Shan QING, Xiaohui ZHANG*, Zhumei LUO, and Xiangdong ZHU

Faculty of Metallurgical and Energy Engineering,
Kunming University of Science and Technology, Yunnan, China

Original scientific paper
https://doi.org/10.2298/TSCI210710337Z

Nanofluids due to their good thermal conductivity and stability, have been proposed as a way to surpass the performance of currently available heat transfer fluids in the near future. In this work, we focuses on the preparation of nanofluids with excellent stability and thermal conductivity, which a new type of stable bismuth iodate oxide ($BiOIO_3$) (one type of infrared non-linear optical crystal) nanofluids is successfully prepared by using the two-step method. After the initial physical characterization of $BiOIO_3$ particles, five different dispersants are used to disperse the $BiOIO_3$ nanoparticles, and the best performing nanofluids with a zeta potential value of 144.45 and an average particle size of 22.90 nm could be prepared with PVP dispersant. Furthermore, the addition of PVP dispersant in UV-visible experiments smooth the light absorption curve of the nanofluids, reach a peak of 1.1 at around 350 nm. In the most important thermal conductivity test, the value of thermal conductivity of $BiOIO_3$ nanofluid becomes larger with increasing concentration at 50 °C, reaching a maximum value of 1.52 at 0.134 vol.%, which increases by 0.72 over the same volume concentration of TiO_2, indicating the importance of the laminar structure. In view of the excellent properties, new laminar structured nanofluids with light-absorbing properties are expected to receive more attention and exploration in the future.

Key words: *$BiOIO_3$ nanofluids, dispersants, UV-visible, thermal conductivity*

Introduction

A new type of heat transfer fluid called *nanofluids* is known to enhance the performance of heat exchange. Nanofluids are two-phase fluids in which solid nanoparticles are immersed in the base fluid and their thermal conductivity can be enhanced by the mixing to improve the heat transfer performance of conventional fluids [1, 2]. In the previous decade, nanofluids have achieved considerable devotion and become a research hotspot due to their enhanced thermal conductivities [3].

In the field of nanofluids research, TiO_2 nanofluids have been widely studied for its high thermal conductivity and easy preparation. Kilic *et al.* [4] performed an experimental study on the effect of TiO_2 nanoparticle addition on the thermal efficiency of flat plate solar collectors. The experiments were conducted in 0.2 wt.% nanofluids with a flow rate of 0.033 kg/s. The results showed that replacing pure water with nanofluids resulted in a 34.45% increase in thermal efficiency. Zhang *et al.* [5] explored the effect of pH on the stability of TiO_2-water

* Corresponding author, e-mail: 54607469@qq.com

nanofluids, and furthermore evaluated the effect of pH-induced stability on dynamic viscosity and thermal conductivity. Said *et al.* [6] revealed that with the addition of TiO_2 nanoparticles volume fraction from 0.1-0.3%, the thermal efficiency of flat-plate solar collectors increased by up to 56%.

The $BiOIO_3$ is a new type of bismuth-based photocatalyst that exhibits excellent photocatalytic performance compared with the commonly used photocatalyst TiO_2 (P25). It is shown that the excellent photocatalytic activity of $BiOIO_3$ is due to its layered structure and internal polarity, both of which facilitate the separation of photogenerated hole electron pairs, thus enhancing the photocatalytic activity. Juyeong *et al.* [7] have investigated the energetics and the physical properties of $BiOIO_3$ based on first-principles calculations. The relationship of the distortion modes to the structural phase transition and the physical properties of the polar phase have been presented. Cui *et al.* [8] have prepared the $BiOIO_3$ nanoplates by a hydrothermal process successfully, the crystallinity and photocatalytic activity of the samples were significantly affected by the temperature, the $BiOIO_3$ prepared at 130 °C displayed the highest photocatalytic activity, and almost all of the RHB was decomposed within 80 minutes. Dong *et al.* [9] combined optical measurements and DFT calculations to verify that $BiOIO_3$ is an indirect gap semiconductor with a band gap of 2.91 eV. Moreover, photocatalytic degradation tests showed that $BiOIO_3$ exhibited excellent photocatalytic performance for the degradation of methyl orange under UV-visible is irradiation, which was much better than its counterparts BiOI and P25.

Among the photocatalytic fields, the nanoscale platelet-like morphology has the special advantage of a shorter carrier diffusion distance, which enables the carrier to reach the reactive site on the surface within its lifetime [10]. In common with TiO_2, $BiOIO_3$ is an excellent photocatalytic material and has a remarkable layered structure, there are no reports on the preparation of nanofluids and further investigation of their thermophysical properties. For these reasons, we have prepared $BiOIO_3$ nanofluids with good stability and thermophysical properties by using $BiOIO_3$ nanoparticles as raw materials and trying to disperse them using five different dispersants, and these properties have been analyzed carefully and systematically. More attention and research on new sheet-like, light-absorbing properties nanofluids are also expected in the future.

Experimental section

Instrument and equipment

The crystal structure and phase purity of the samples was determined by XRD (Bruker D8 Advance, Germany) using Cu Kα radiation, and the scanning range was 10-100° (2θ). The morphologies and structures of asprepared samples were observed by SEM (S-4800 Hitachi, Japan), and the diffuse reflectance absorption spectra (DRAS) were obtained with the UV-visible spectrophotometer (UV-3900H, Hitachi, Japan). The Zeta potential and average grain size distribution were obtained by NanoBrook 90 plus Zeta analyzer (Brookhaven Instruments Corporation, USA). The measurements against the heat transfer coefficient was used the Hot Disk method (TPS2500S, Sweden).

Preparation of powder sample

The $BiOIO_3$ powder samples are prepared by using a simple hydrothermal process and all of the chemicals used in the experiment were analytical grade reagents without further purification. The $Bi(NO_3)_3{\cdot}5H_2O$ and KIO_3 were used as the sources of Bi and IO_3 so that to synthesize the $BiOIO_3$ sample. At first, 1 mmol of $Bi(NO_3)_3{\cdot}5H_2O$ was dissolved in 40 mL of deionized water to form a suspension after constant stirring (400 rpm for 5 minutes used the magnetic stirrer). Secondly, 1 mmol of KIO_3 was added into the suspension under vigorous stirring (750 rpm for 6 minutes). The mixture was transferred into 100 mL Teflon-lined stainless steel autoclaves [9]. The aqueous suspension was hydrothermally heated at a temperature of 150 °C. After five hours, the samples naturally cooled to room temperature. Then, all generated samples were obtained by centrifuging them, filtering them, and rinsing them with deionized water and ethanol for four times. At last, the samples were dried at 60 °C for 12 hours and grinded into powder samples.

Preparation of powder nanofluids

The preparation of nanofluids can be divided into one-step and two-step methods [11]. The two-step method involves the synthesis of nanoparticles firstly, which are dispersed in the liquid, and the stability of the nanofluids is maintained by the dispersant [12]. So in this paper, Two-step method is used to prepare $BiOIO_3$-water nanofluids with the grinded powder samples and various dispersing agent which playing a good dispersion effect can slow down the deposition of nanoparticles to a certain extent.

In order to prepare the $BiOIO_3$ nanofluids with excellent stability, and explore the dispersion effect of various dispersants, we have designed two groups of preparation experiment. In the first of group, the mass fraction of the dispersants in prepared nanofluids samples are 0.5 wt.% and the $BiOIO_3$ powder samples were 0.3 wt.%. The kinds of dispersants added were SDBS, PVP, TMAH, SDS, and CTAB, respectively. The weighed dispersants was added to the nanoparticle mixture with the working medium deionized water. Then, 15 minutes magnetic stirring was adopted to get the evenly mixed nanofluids, after that we placed the uniformly mixed nanofluids suspension in the ultrasonic vibration tank for 30 minutes, and took it out for subsequent experiments finally.

After a series of experiments, we established the superiority of the PVP dispersant, thus, in the second of group, the mass fraction of the dispersants in prepared nanofluids samples are 0.5 wt.% and the $BiOIO_3$ powder samples were 0.1, 0.3, 0.5, 0.8, and 1.0 wt.%, respectively. So that we could compare the properties of nanofluids with different dispersant concentrations under the background of the same dispersant ratio.

Results and discussions

Property characterization of $BiOIO_3$

In the first step, the XRD patterns of as-prepared $BiOIO_3$ samples was shown in fig. 1. The characteristic diffraction peaks of $BiOIO_3$ accorded well with the database of ICSD No. 262019 (the specific value of the diffraction peak has been marked in detail in the figure), which fitted with the card exactly, demonstrating the pure phase of $BiOIO_3$. No other peaks were found suggesting the high purity and crystallinity of the sample.

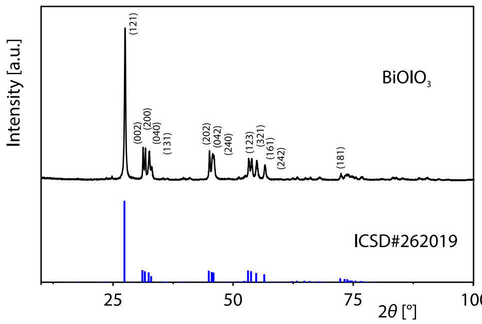

Figure 1. The XRD of as-prepared $BiOIO_3$ samples

The particle size and morphology of $BiOIO_3$ products were observed by the field emission SEM. As shown in fig. 2, the $BiOIO_3$ samples showed clear lamellar morphology, which was similar to those of other $(Bi2O_2)^{2+}$ layer-containing compounds [13]. The samples presented a flake stack morphology, which has an average width around 150 nm and the thick-

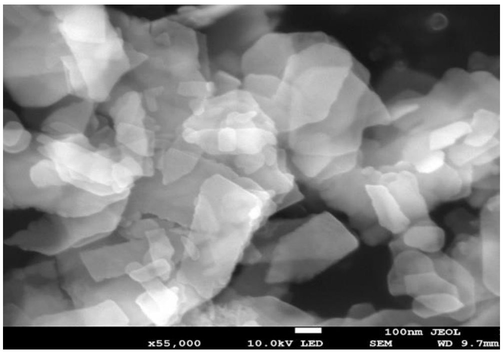

Figure 2. The SEM of $BiOIO_3$ samples

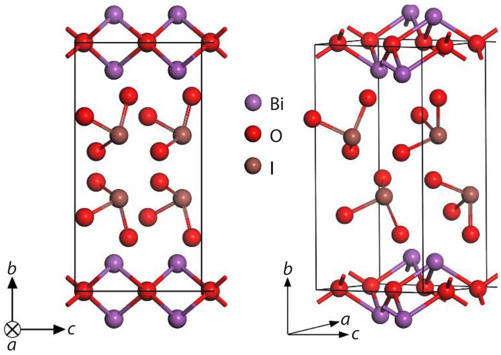

Figure 3. Crystal structure of $BiOIO_3$

ness of the $BiOIO_3$ sample was estimated to 40 nm. And the specific surface area of the pristine $BiOIO_3$ was measured, which was calculated to be 11.281 m^2/g.

From the perspective of crystal structure, as shown in the fig. 3, it was observed that the crystal structure of BiOIO3 shows a laminar distribution, which was the fundamental reason for the laminar accumulation of particles. In the figure, BiO_6 and IO_3 polar groups were connected by bridge oxygen atoms to form the 3-D structure, while $(Bi2O_2)^{2+}$ was connected to the upper and lower layers of $(IO_3)^-$ by bridge oxygen atoms, respectively. In general, a multilayer arrangement structure was formed in the ac plane in the perpendicular direction the *b*-axis, and its microscopic layer structure determined its macroscopic morphology as a lamellar crystal. This was the unique feature of layered compounds, which had been reported previously in the literature to easily synthesize similar morphologies [14].

In the field of photocatalysis research, nanoscale sheet morphology with short carrier diffusion distance, which enables the carrier to reach the reactive site on the surface within its lifetime. In addition, the thickness of the layered photocatalytic material is also an important factor affecting the photocatalytic performance. But now, more importantly, the laminate structure also has an important effect on the thermal conductivity, which is the main direction and starting point of this paper's research. Further exploration and research on the thermal conductivity of $BiOIO_3$ nanofluids will also be carried out in this paper.

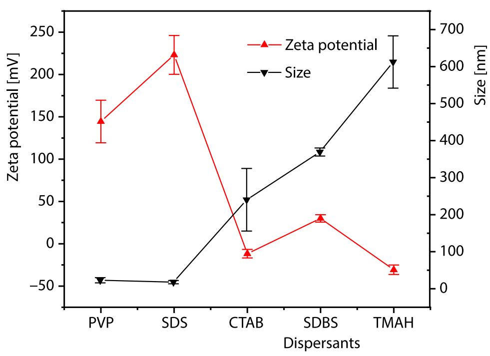

Figure 4. Particle size and Zeta potential of $BiOIO_3$ nanofluids prepared by different dispersants

Zeta potential and particle size analysis

In nanofluidic systems, it would be easier to form large size agglomerates due to the greater surface energy, and the addition of additives could result in greater dispersion, which would lead to smaller average size of such particle agglomerates [15]. As could be seen from the fig. 4 that the $BiOIO_3$ nanofluids prepared by five different dispersants (PVP, SDS, CTAB, SDBS, and TMAH), their average particle size (in fact the average size of particle agglomerates) and Zeta potential were different obviously. The absolute values of Zeta potential of PVP and SDS were the largest (the specific values were 144.45 and 223.17, and the values of the three remained dispersants were CTAB 11.68, SDBS 30.00, and TMAH 30.70), which indicated that the surface enrichment of nanoparticles in water had more charges and the repulsive force between the particles was larger, making the nanofluids dispersion more stable [16]. Based on the potentiometric analysis, PVP and SDS were the ideal dispersants for the experiment, and then we continued to analyze the effect of particle size.

Equally and significantly, the particle size of $BiOIO_3$ nanoparticles was also an important criterion. As can be seen from the graph, the SDS particle size 17.83 nm was the smallest (particle size of the remaining four dispersants PVP 22.90 nm, CTAB 240.27 nm, SDBS 369.17 nm, and TMAH 612.39 nm). In the aforementioned data, these two properties Zeta potential and particle size, were similar for SDS and PVP relatively, which prevented us from drawing qualitative conclusions. So we required stability experiments to observe the homogeneity of the nanofluids. In our subsequent studies, it would be beneficial to conduct in-depth studies on the effects of dispersants on light absorption and heat transfer.

Stability characterization of nanofluids

As observed in fig. 5, the $BiOIO_3$ nanofluids added with different additives had different suspensions occurring 2 hours after the completion of preparation (quality fraction of the dispersant in nanofluids was 0.5 wt.% and 0.3 wt.% for $BiOIO_3$ powder samples), a significant sedimentation occurred in SDBS and TMAH, and the delamination of the remaining three was not obvious.

In the observation photos of the next few days, we could find that all of the nanofluids underwent significant sedimentation with the exception of two nanofluids, PVP and SDS, which remained partially suspended, this was especially apparent in the photos after 14 days. Compared with the nanofluids after the action of SDS and PVP, it was obviously found that PVP performed better, especially in the 7 days and 14 days photos, the color of aggregations of PVP added nanofluids are lighter than nanofluids prepared by adding SDS dispersing agents. In summary, sample of PVP maintained a good suspension stability in the 14 days photo, which was conducive to the further exploration of the subsequent tests.

In combination with the previous experiments, we decided to do special experiments on nanofluids prepared by PVP additive in order to explore the stability of nanofluids under different particle concentration conditions.

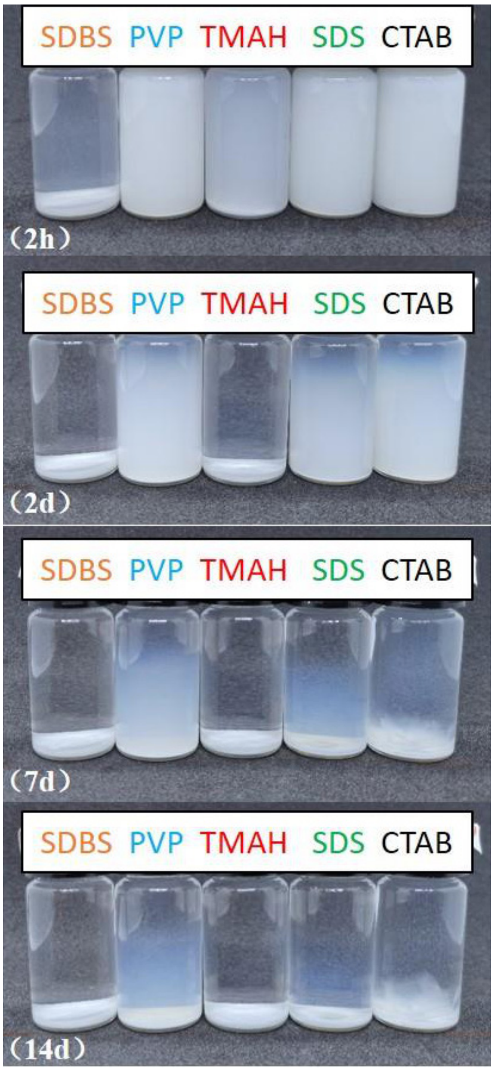

Figure 5. The sedimentation photography of different additives

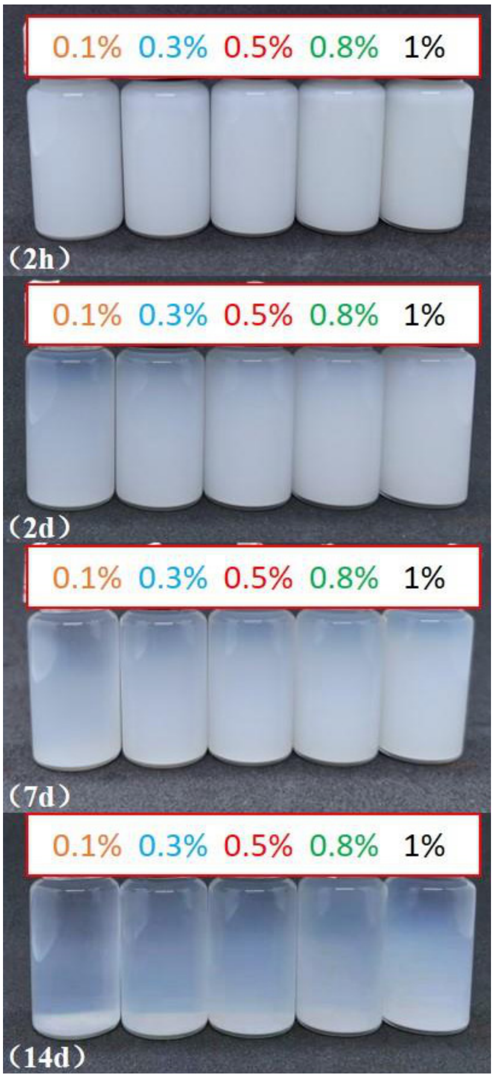

Figure 6. The sedimentation photography of PVP additive hy of different additives

The photographs of the nanofluids formed by the preparation at a dispersant amount of 0.5 wt.% and nanoparticles of 0.1, 0.3, 0.5, 0.8, and 1.0 wt.% separately, after being rested for different times, were shown in fig. 6. As observed in the figure, the color of the samples has always gradually become darker in the photos at each time point, and the stability of the nanofluids exhibited a regular distribution with the change of concentration [17]. From the photos after 14 days, it was evident that the samples were still stable, indicating that the nanofluids prepared with PVP as an additive was usable and stable, which was a valid guide for our light absorption experiments and thermal conductivity studies.

The UV-visible light absorption properties

The UV-visible DRAS of $BiOIO_3$ was displayed in fig. 7(a). In the small diagram in the upper right corner of the figure, a comparison of the light absorption of TiO_2 and $BiOIO_3$ powders were demonstrated, and it could be seen that the absorption edges of both were basically the same, located around 395 nm. According to the eq. (1), the band edge wavelength, λ_g, is determined by the forbidden band width, E_g [eV] [18], it could be deduced that the forbidden band width of $BiOIO_3$ sample was around 3.10 eV, which was higher than the general photocatalyst, similarly, closed to TiO_2 (3.06 eV), and this result was in accordance with the previous literature reports. Moreover, this observation clearly demonstrated that BiOIO3 is an UV-driven photocatalyst, mainly due to the large band gap of $BiOIO_3$, which leads to its light absorption range falling within the UV-absorption spectrum and the larger light wavelength required to achieve catalysis:

$$E_g = \frac{1240}{\lambda_g} \tag{1}$$

As shown in fig. 7(a), we took the supernatant from the prepared various $BiOIO_3$ stable nanofluids for the DRAS testing (five types of dispersants were added and the nanofluids were stably suspended after 7 days with formulations of 0.5 wt.% dispersant and 0.3 wt.% $BiOIO_3$ powders). It was consistent with the results of stability experiments in the previous section that PVP, represented by the red line, performed the best, with its visible light absorption started from 800 nm, slowly increased and continued to absorb light, and reached a peak of 1.1

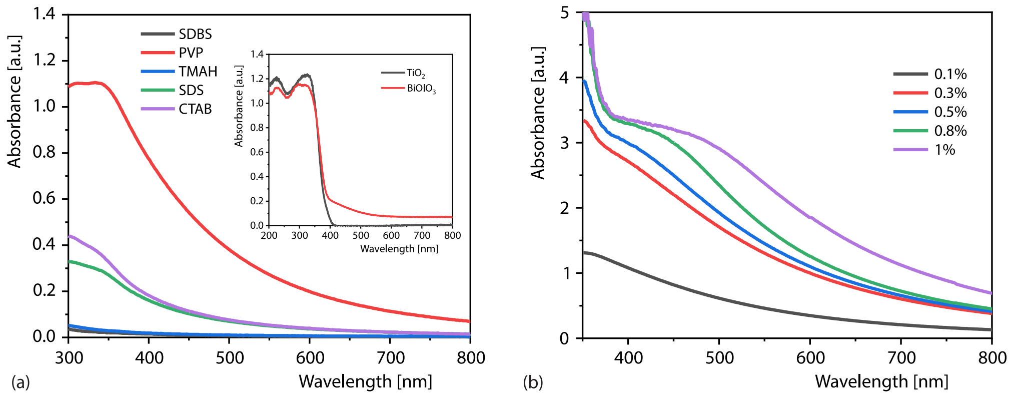

Figure 7. The UV-visible DRAS of $BiOIO_3$ and related samples; (a) five different types of dispersants and the small diagram shows the comparison of TiO_2 and $BiOIO_3$ powders and (b) five different concentrations (*for color image see journal web site*)

at around 350 nm, with the strongest absorbance performance, and this value was about 0.65 higher compared to other dispersants. In summary, the best absorbance of nanofluids under the action of PVP dispersant also confirmed the best dispersion of PVP, which allowed the nanoparticles to be uniformly dispersed in water. There remained an interesting phenomenon worth noting, the addition of different kinds of dispersants resulted in smoother light absorption curves compared to nanoparticles. It was attributed to the fact that the dispersants could broaden the spectral absorption range effectively, and in detail the enhanced dispersion of the nanofluids increased the concentration of the liquid irradiated by the spectrum [19], which enhanced the light absorption capacity of the nanofluids ultimately.

In order to highlighted the effect of concentration on absorbance, unlike the aforementioned experiments where stable suspensions were selected after 7 days, in this experiment, we compared the PVP dispersant nanofluids after two hours of preparation completion directly (the middle suspension of the test tube was selected). The UV-visible spectrophotometer work between visible and UV-spectra. The light with fixed intensity and wavelength emitted from the emitter will be attenuated by the intensity received at the receiver after passing through a glass dish of equal thickness, and the concentration of the solution will be effectively reflected by calculating the percentage of attenuation [20].

In fig. 7(b), it indicated that the light absorption curves of nanofluids with different concentrations after adding 0.5 wt.% PVP dispersant, it was observed that the height of the light absorption curves increased sequentially with the increasing mass concentration of $BiOIO_3$ sample. At 395 nm position, the absorbance of 1% concentration was stabilized at 3.378. The absorbance of the remaining 0.8%, 0.5%, 0.3%, and 0.1% concentrations were 3.314, 3.036, 2.754, and 1.109, respectively. In summary, the absorbance curves of different concentrations of nanofluids were significantly different, and there was a clear pattern of increasing absorbance values with increasing concentrations. This pattern also provided a basis for the subsequent thermal conductivity study.

Thermal conductivity of $BiOIO_3$ nanofluids

In the thermal conductivity test, we compared $BiOIO_3$ nanofluids after 2 hours of preparation completion with nanoparticles added with different mass fractions in the presence of 0.5 wt.% PVP dispersant.

The addition of nanoparticles can significantly improve the thermal conductivity of the fluids for the following three reasons: first, when nanoparticles perform irregular motion in the fluid, the energy carried by the particles migrates, and this energy migration enhances the energy transfer inside the nanofluids and improves the thermal conductivity of the nanofluids [21], secondly, the micro-motion of nanoparticles enables the existence of micro-convection between the particles and the liquid, which enhances the energy transfer between the particles and the liquid as well as improves the thermal conductivity of the nanofluids, and last but not least, nanoparticles increase the heat capacity and surface area of solid-liquid phase of heat transfer fluid, which increases the thermal conductivity of fluid as well as enhances the interaction and collision between particles and particles, particles and liquid in addition particles and walls, resulting in stronger heat transfer [22].

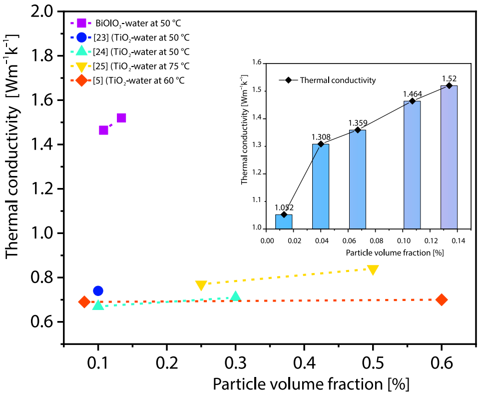

Figure 8. Thermal conductivity of $BiOIO_3$ and TiO_2

In terms of thermal conductivity studies, we mainly selected TiO_2 as a comparator because it has been studied for a long time and its good thermal conductivity properties have also been consistently recognized in the nanofluids neighborhood for its mature and widespread applications. The distribution of TiO_2 thermal conductivity in some recent studies were shown in fig. 8. Wang's [23] study showed that the thermal conductivity of TiO_2-water nanofluids was 0.74 °C at 50 °C, 0.1 vol.% concentration. Said *et al.* [24] in their study found that the thermal conductivity of TiO_2-water nanofluids at 50 °C, 0.1 vol.% and 0.3 vol.% concentration were of 0.67 and 0.71. Meanwhile, Bakhtiari *et al.* [25] in their latest study found that thermal conductivity at 0.25 vol.% and 0.5 vol.% concentrations exhibited 0.77 and 0.84, respectively, in the background of 55 °C. Most importantly, in the previous in-depth study of TiO_2 nanofluids by our research group Zhang *et al.* [5] the thermal conductivity was found to be 0.69 and 0.70 at 0.08 vol.% and 0.6 vol.% concentrations at 60 °C, respectively, which was outstanding in the same kind of study.

For the accuracy of the comparison of experimental results, we referred to the value of $BiOIO_3$ density of 7.44 g/cm^3 reported by previous scholars, and converted the mass concentration volume concentration in this paper in the case of convenient comparison. Figure 8 revealed that the thermal conductivity of $BiOIO_3$ was significantly improved compared to TiO_2 under the same conditions, where the thermal conductivity at 0.107 vol.% and 0.134 vol.% concentrations at 50 °C exhibited 1.46 and 1.52, respectively, which was an improvement of 0.72 compared to Wang's [23] TiO_2-water nanofluids thermal conductivity of 0.74 at the same conditions of 0.10 vol.%. The improvement was as much as 97%, which was a great and significant improvement.

In the small diagram in the upper right corner of fig. 8, we illustrated the thermal conductivity *vs.* concentration at 50 °C completely. The thermal conductivity of the nanofluids at 1% mass concentration was stable at 1.520, the remaining 0.8%, 0.5%, 0.3%, and 0.1% concentrations had thermal conductivities of 1.464, 1.359, 1.308, and 1.052, respectively. It could be seen that the thermal conductivity tends to increase with the enhancement of concentration, and there was a large improvement in the value compared with TiO_2-water nanofluids.

Analyzing the reason, we concluded that apart from its own physical properties such as $BiOIO_3$ density, its laminar structure was the key factor for its thermal conductivity enhancement, which analogously was 17.5% higher for graphene nanofluids with the same laminar structure than itself other columnar, flower-like structure. Overall, the thermal conductivity of nanofluids depends on the combined effect of effective thermal diffusion and particle migration of solid and liquid phases [26], nanofluids with large specific surface area, particle-particle, solid-liquid collision is stronger, which means that the role of particle migration is larger, the liquid film layer attached to the surface of two particles will be in contact or partially overlapped area will be significantly increased, so that the thermal short circuit of the heat transfer process occurs, and forcing the thermal resistance to decrease significantly, which eventually leads to the enhancement of the effective thermal diffusion of the solid-liquid two-phases of the suspension and the increase of the effective thermal conductivity.

Conclusions

In this paper, we used the excellent crystal $BiOIO_3$ as a raw material for nanofluids and dispersed it with five different kinds of dispersants, expecting to prepare $BiOIO_3$ nanofluids with good stability and thermophysical properties.

First of all, we characterized the physical properties of the initially prepared $BiOIO_3$ powder and determined that pure $BiOIO_3$ without other heterogeneous phases was prepared by observing the XRD patterns. Subsequently, it was observed in depth using SEM to characterize its morphological features with the width of 150 nm, thickness of 40 nm and specific surface area of 11.281 m^2/g. After that, the two-step method was used to prepare stable $BiOIO_3$-water nanofluids for the first time.

During the next experiments, the nanofluids were prepared and tested with five different dispersants using a combination of Zeta potential and particle size tests, and the most favorable data were found with the addition of PVP and SDS, with PVP having a Zeta potential value of 144.45 and a particle size of 22.90 nm. The observations from stability experiments showed that PVP maintained good stability, with the least significant settling in the 14 day resting experiment. The sedimentation was the least obvious in the 14 day resting experiment. The analysis of the previous experimental results concluded that the nanofluids prepared with PVP has the best stability.

In the UV-visible experiments, we compared the light absorption effect of nanofluids with the addition of five dispersants, and in accordance with the previous experimental results PVP performed the best, and the addition of dispersant made the light absorption curve of nanofluids smoother and reached a peak of 1.1 at around 350 nm. The peak of absorbance increased with the increase of $BiOIO_3$ mass concentration under the effect of PVP additive.

Based on the aforementioned UV-visible experiments, we conducted in-depth thermal conductivity tests on nanofluids with different $BiOIO_3$ particle concentrations, and the results showed that the thermal conductivity of $BiOIO_3$ nanofluids gradually increased with increasing concentration under 50 °C test conditions, and the highest value of 1.520 was achieved at 0.134 vol.%. In comparison with the same volume concentration of TiO_2, we found that the thermal conductivity increased by 0.72 compared to TiO_2 under the same conditions, and the explanation revealed that the laminar structure played a significant role.

As a result of this paper, $BiOIO_3$ not only possesses good photocatalytic properties, but also has good light absorption properties and excellent thermal conductivity when prepared as stable nanofluids. Moreover, the $BiOIO_3$ sheet-structured nanomaterial itself, due to its uniform structural size, large specific surface area and good absorption effect, has a strong ability to capture light energy. Therefore, it is of great significance to study the sheet-structured $BiOIO_3$ nanofluids in terms of heat conduction transport and its application in the field of photo-thermal conversion. We also hope that the new lamellar, and $BiOIO_3$ nanofluids with light absorption properties together with its similar nanofluids will obtain more attention as well as greater development in the future.

Acknowledgment

This work were supported by National Natural Science Foundation of China under Contract (No. 52069010 and 51966005) and Yunnan Fundamental Research Projects (No. 202101AT070120).

Reference

[1] Maxwell, J. C. A., A Treatise on Electricity and Magnetism, *Nature*, (1981), *7* (182), pp. 478-480
[2] Wang, B. X. Effect of Particle Agglomeration on Thermal Properties and Thermal Process of Low Concentration Nanofluids, *Journal of Mechanical Engineering*, *45* 2009), 3, pp. 1-4
[3] Zhang, R. H., *et al.*, Research on Convective Heat Transfer Characteristics of Fe_3O_4 Magnetic Nanofluids under Vertical Magnetic Field, *Thermal Science*, *26* (2022), 18, pp. 667-679
[4] Kilic, F., *et al*., Effect of Titanium Dioxide-Water Nanofluid Use on Thermal Performance of the Flat Plate Solar Collector, *Solar Energy*, *164* (2018), Apr., pp. 101-108
[5] Zhang, H., *et al.*, The Changes Induced by pH in TiO_2-Water Nanofluids: Stability, Thermophysical Properties and Thermal Performance, *Powder Technology*, *377* (2021), Jan., pp. 748-759
[6] Said, Z., *et al*., Performance Enhancement of a Flat Plate Solar Collector Using Titanium Dioxide Nanofluid and Polyethylene Glycol Dispersant, *Journal of Cleaner Production*, *92* (2015), Apr., pp. 343-353
[7] Kim, J., *et al*., Electronic Structure and Polarization of Polar $BiOIO_3$, *Journal Korean Physical Society*, *75* (2019), 12, pp. 990-996
[8] Cui, D. H., *et al*., Hydrothermal Synthesis, Characterisation and Photocatalytic Properties of $BiOIO_3$ Nanoplatelets, *Journal of Experimental Nanoscience*, *11* (2016), 12, pp. 1000-1010
[9] Dong, X. D., *et al*., Spontaneous Polarization Effect and Photocatalytic Activity of Layered Compound of $BiOIO_3$, *Inorganic Chemistry, 58* (2019), 22, pp. 15344-15353
[10] Liu, Y., *et al*., The 2-D SnS_2 Nanosheets Exfoliated from an Inorganic-Organic Hybrid with Enhanced Photocatalytic Activity Towards Cr(VI) Reduction, *Inorganic Chemistry Frotiers*, *6* (2019), 4, pp. 948-954
[11] Ahmed, Z., *et al*., A Molecular Dynamics Approach of the Effect of Thermal Interfacial Resistance and Nanolayer on Enhanced Thermal Conductivity of Al_2O_3-CO_2 Nanofluid, *Journal of Enhanced Heat Transfer*, *28* (2021), 2, pp. 41-56
[12] Alous, S., *et al*., Experimental Study about Utilization of MWCNT and Graphene Nanoplatelets Water-Based Nanofluids in Flat Non-Concentrating PVT Systems, *Thermal Science*, *25* (2021), 1B, pp. 477-489
[13] Sun, Y., *et al*., Interlayer-I-Doped $BiOIO_3$ Nanoplates with an Optimized Electronic Structure for Efficient Visible Light Photocatalysis, *Chemical Communications*, *52* (2016), 53, pp. 8243-8246
[14] Sun, X., *et al.*, Fabrication of $BiOIO_3$ with Induced Oxygen Vacancies for Efficient Separation of the Electron-Hole Pairs, *Applied Catalysis B: Environmental*, *218* (2017), Dec., pp. 80-90
[15] Qiu, L., *et al*., A Review of Recent Advances in Thermophysical Properties at the Nanoscale: From Solid State to Colloids, *Physics Report*s, *843* (2020), Feb., pp. 1-81
[16] Toghraie, D., *et al*., Measurement of Thermal Conductivity of ZnO-TiO_2-EG Hybrid Nanofluid, *Journal of Thermal Analysis and Calorimetry*, *125* (2016), 1, pp. 527-535
[17] Bahiraei, M., *et al*., Application of an Ecofriendly Nanofluid Containing Graphene Nanoplatelets Inside a Novel Spiral Liquid Block for Cooling of Electronic Processors, *Energy*, *218* (2021), Mar., 1119395
[18] Salari, A., *et al.*, Nanofluid Based Photovoltaic Thermal Systems Integrated with Phase Change Materials: Numerical Simulation and Thermodynamic Analysis, *Energy Conversion and Management*, *205* (2020), Feb., 112384
[19] Salari, A., *et al*., An Updated Review of the Performance of Nanofluid-Based Photovoltaic Thermal Systems from Energy, Exergy, Economic, and Environmental (4E) Approaches, *Journal of Cleaner Production*, *282* (2020), Feb., 124319
[20] Jia, Y., *et al*., Numerical Analysis of Photovoltaic-Thermal Collector Using Nanofluid as a Coolant, *Solar Energy*, *196* (2020), Jan., pp. 625-636

[21] Dagdevir, T., *et al*., Optimization of Process Parameters in Terms of Stabilization and Thermal Conductivity on Water Based TiO_2 Nanofluid Preparation by Using Taguchi Method and Grey Relation Analysis, *International Communications in Heat and Mass Transfer*, *120* (2020), Jan., 1050047
[22] Rahmati, M., Effects of ZnO-Water Nanofluid on the Thermal Performance of Wet Cooling Towers, *International Journal of Refrigeration*, *131* (2021), Nov., pp. 526-534
[23] Wang, Y., *et al*., Improving Stability and Thermal Properties of TiO_2 Nanofluids by Supramolecular Modification: High Energy Efficiency Heat Transfer Medium for Data Center Cooling System, *International Journal of Heat and Mass Transfer*, *156* (2020), 119735
[24] Said, Z., *et al*., New Thermophysical Properties of Water Based TiO_2 Nanofluid – The Hysteresis Phenomenon Revisited, *International Communications in Heat and Mass Transfer*, *58* (2014), Nov., pp. 85-95
[25] Bakhtiari, R., *et al*., Preparation of stable TiO_2-Graphene-Water Hybrid Nanofluids and Development of a New Correlation for Thermal Conductivity, *Powder Technology*, *385* (2021), June, pp. 466-477
[26] Valan, A. A., *et al.*, Experimental Validation of Enhancement in Thermal Conductivity of Titania-Water Nanofluid by the Addition of Silver Nanoparticles, *International Communications in Heat and Mass Transfer, 120* (2021), 6, 104910

Paper submitted: July 10, 2021
Paper revised: October 1, 2021
Paper accepted: October 15, 2021